The Journal of Membrane Biology
https://doi.org/10.1007/s00232-022-00250-0

Trans-Resveratrol Decreases Membrane Water Permeability: A Study of Cholesterol-Dependent Interactions

Jasmin Ceja-Vega[1] · Escarlin Perez[1] · Patrick Scollan[1] · Juan Rosario[1] · Alondra Gamez Hernandez[1] · Katherine Ivanchenko[1] · Jamie Gudyka[1] · Sunghee Lee[1]

Received: 4 January 2022 / Accepted: 28 May 2022
© The Author(s), under exclusive licence to Springer Science+Business Media, LLC, part of Springer Nature 2022

Abstract

Resveratrol (RSV), a biologically active plant phenol, has been extensively investigated for cancer prevention and treatment due to its ability to regulate intracellular targets and signaling pathways which affect cell growth and metastasis. The non-specific interactions between RSV and cell membranes can modulate physical properties of membranes, which in turn can affect the conformation of proteins and perturb membrane-hosted biological functions. This study examines non-specific interactions of RSV with model membranes having varying concentrations of cholesterol (Chol), mimicking normal and cancerous cells. The perturbation of the model membrane by RSV is sensed by changes in water permeability parameters, using Droplet Interface Bilayer (DIB) models, thermotropic properties from Differential Scanning Calorimetry, and structural properties from confocal Raman spectroscopy, all of which are techniques not complicated by the use of probes which may themselves perturb the membrane. The nature and extent of interactions greatly depend on the presence and absence of Chol as well as the concentration of RSV. Our results indicate that the presence of RSV decreases water permeability of lipid membranes composed of 1,2-dioleoyl-*sn*-glycero-3-phosphocholine (DOPC), indicating a capability for RSV in stiffening fluidic membranes. When Chol is present, however, (at 4:1 and 2:1 mol ratio DOPC to cholesterol), the addition of RSV has no significant effect upon the water permeability. DSC thermograms show that RSV interacts with DOPC and DOPC/Chol bilayers and influences their thermotropic phase behavior in a concentration-dependent manner, by decreasing the main phase transition temperature and enthalpy, with a phase separation shown at the higher concentrations of RSV. Raman spectroscopic studies indicate an ordering effect of RSV on DOPC supported bilayer, with a lesser extent of ordering in the presence of Chol. Combined results from these investigations highlight a differential effect of RSV on Chol-free and Chol-enriched membranes, respectively, which results constitute a bellwether for increased understanding and effective use of resveratrol in disease therapy including cancer.

✉ Sunghee Lee
SLee@iona.edu

[1] Department of Chemistry and Biochemistry, Iona College, 715 North Avenue, New Rochelle, NY 10801, USA

Published online: 24 June 2022

Graphical Abstract

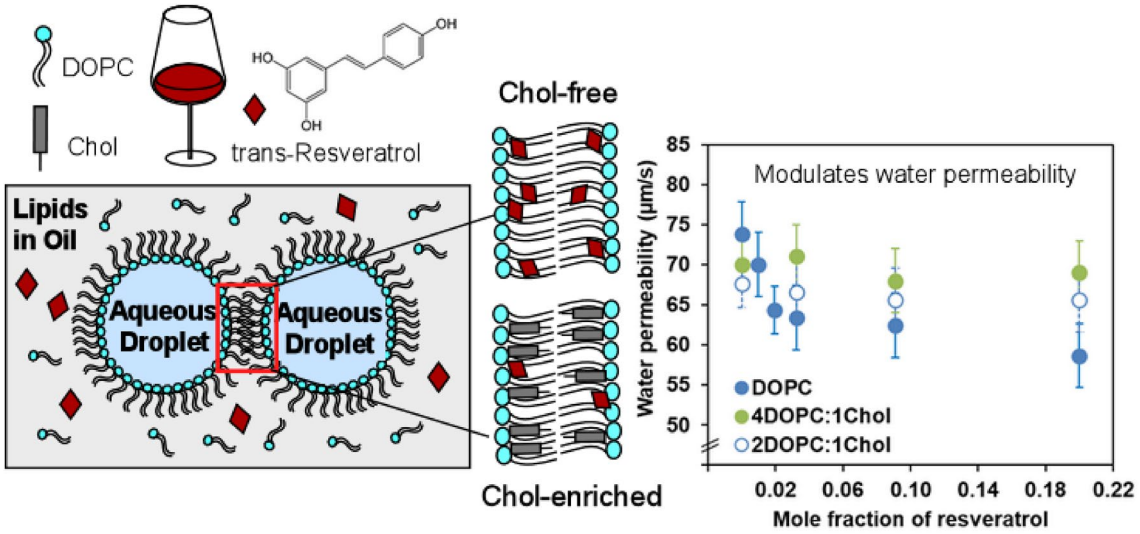

Keywords Resveratrol · Water permeability · Differential Scanning Calorimetry · Confocal Raman Microspectroscopy · 1,2-dioleoyl-*sn*-glycero-3-phosphocholine (DOPC) · Cholesterol

Introduction

Increasing attention has focused upon biologically active phenols for their many beneficial properties, with applications in health and nutrition (Crozier et al. 2009; Quideau et al. 2011; Ramassamy 2006). One of the most widely studied plant-derived polyphenols, *trans*-3,4′,5-trihydroxystilbene, commonly named *trans*-resveratrol (the *trans*-isomer is hereinafter to be referred to simply as RSV), is found in many foods, including grapes and red wine (Crozier et al. 2009; Fulda 2010; Keylor et al. 2015). RSV has been reported to exhibit broad range of beneficial pharmacological activities that lead to potential pleiotropic therapeutic applications, notably as antioxidant, anti-inflammatory, anticarcinogenic, cardioprotective, and neuroprotective agent (Athar et al. 2007; Baur and Sinclair 2006; Berman et al. 2017; Harikumar and Aggarwal 2008; Salehi et al. 2018). Particularly RSV has been shown to protect cellular biomolecules from oxidative damage through its ability of inhibiting or directly neutralizing reactive oxidative species (ROS) (Truong et al. 2018). RSV is known to regulate multiple intracellular molecular targets and signaling pathways which affect cell growth, inflammation, apoptosis, angiogenesis, and metastasis, and has been extensively investigated for cancer prevention and treatment (Jang et al. 1997; Ko et al. 2017; Kundu and Surh 2008). It is reported that RSV alters the function of a wide spectrum of unrelated proteins including transmembrane proteins that are implicated in RSV biological effects, but few binding sites that account for its effectiveness have been identified (Ingólfsson et al. 2014; Pavan et al. 2016; R Neves et al. 2012). Therefore, it has become increasingly recognized that many effects of RSV could stem from the non-specific interaction with the biological membranes, in addition to its direct effect on specific molecular targets (Baell 2016; Ingólfsson et al. 2014; R Neves et al. 2012). These beneficial effects, usually demonstrated in vitro, must, however, be tempered by the fact that RSV is quickly metabolized in vivo, bringing a measure of uncertainty as to the physiological relevance of the concentrations used for in vitro experiments (Baur and Sinclair 2006). Many biological processes are mediated by lipid bilayer membrane-bound proteins, which require an adequate membrane matrix to ensure their structural and functional integrity (Andersen and Koeppe 2007; Phillips et al. 2009). It has been demonstrated that lipid bilayers play a critical role in the physiological activity of membrane proteins. The perturbation of the physicochemical properties of their host lipid bilayer membrane, driven by exogenous molecules via non-specific interactions, can influence protein conformation and in turn the functioning of embedded proteins, which can lead to significant changes in their biological functions of homeostasis maintenance, protein activity and propagation of cellular signaling processes (Ingólfsson et al. 2014; Lundbæk et al. 2010). For example, it was reported that the ability of RSV to inhibit protein kinase C, a membrane-dependent enzyme involved as a regulatory element in the modulation of a variety of cellular processes such as cell signaling and tumor promotion, is due in part to

the interaction of the protein with the lipid bilayer (García-García et al. 1999). Previous studies have shown that non-specific interactions between RSV and the lipid bilayer membranes can lead to modulation of collective membrane properties, such as biomechanical, structural, electrical and thermodynamic properties. These types of reorganizations of membrane physical properties are known to play an important role in physiological functions, including cell fusion, cell division, endocytosis, and exocytosis.

Cholesterol (Chol) is one of the most important components of animal cell membranes, comprising a high fraction of total lipid in the plasma membrane (ca. 20–50 mol%), and a much smaller fraction in intracellular components, e.g., 3 wt.% in mitochondria (Mouritsen 2005). The major role of Chol in the membrane has been considered as principally in its ability to impart order upon the lipidic array of the membrane, to thereby modulate the structural and physicochemical properties of the plasma membrane lipid bilayer, and as a result, regulating the function of a wide range of trans-membrane proteins (Ohvo-Rekilä et al. 2002; Yeagle 1991). Chol is also a key component of lipid rafts (Brown and London 2000), considered the major platforms for signaling regulation in cancer and essential for oncogenic signals (Ding et al. 2019). Changes in membrane Chol have been shown to affect cancer progression and immune responses (Ding et al. 2019; Huang et al. 2020), and its metabolism is frequently altered in cancer cells resulting in either lower or higher values of Chol that may vary according to the type of cancer and its stage and sensitivity (Alves et al. 2016; Zalba and Ten Hagen 2017). It has been reported that RSV accumulates in lipid rafts prior to its endocytosis, based on a study using the uptake of radiolabeled RSV in colon cancer cells and leukemia cell lines, thereby confirming the importance of lipid rafts in the biological effects of resveratrol (Colin et al. 2011; Delmas et al. 2013). It is seen that cancer cells preparing for metastasis reduce membrane Chol content to enhance their membrane fluidity and plasticity, which is essential for their penetration of blood vessels (Szlasa et al. 2020), but higher values of Chol can be found in multidrug resistant cells, presumably due to the membrane being more rigid and thus less permeable for drugs (Szlasa et al. 2020).

The essential scaffolding of a biological membrane is its lipid bilayer, which forms a protective hydrophobic barrier between the endocellular compartment and its surroundings (Stillwell 2013). The composition of various cell membranes consists of a rich mixture of highly diverse constituents such as lipid, carbohydrates, and proteins (Van Meer et al. 2008). The lipid species alone differ in terms of their headgroup, chain length, and degree & position of unsaturation of hydrocarbon chain (Stillwell 2013). Owing to to the complex natureof the cellular membrane, lipid membrane modelss have been developed to foster investigation of the role of lipids in the interactions between drugs and membranes in a controllable manner (Rosilio 2018). One such model membrane is the droplet interface bilayer (DIB), which is engineered by contact of two lipid monolayer-coated aqueous droplets in an hydrophobic oil medium. The contact region comprises a lipid bilayer. This bilayer mimics the two leaflets of the cellular membrane bilayer structure, as shown in Fig. 1 (Funakoshi et al. 2006; Holden et al. 2007). In our earlier studies, we have established that a DIB is a convenient and reliable membrane mimetic system to readily explore passive membrane water transport (Michalak et al. 2013; Milianta et al. 2015), a phenomenon which plays a significant role in cellular physiology and maintaining homeostasis. In addition, water permeability has been suggested to constitute a measure to assay membrane stability for ionic leakage, since water penetration assists hydrophilic moieties such as ions to permeate the lipid membrane (Shinoda et al. 2008). Given that the water transport process is a function of the underlying physical state of the lipid bilayer and its structure (Hill and Zeidel 2000), it has been desirable to establish a consistent and reliable platform for quantifying water transport through bilayers, as a means to shed light on bilayer physical properties. Towards this, our previous investigations provide ample demonstration of how self-assembly

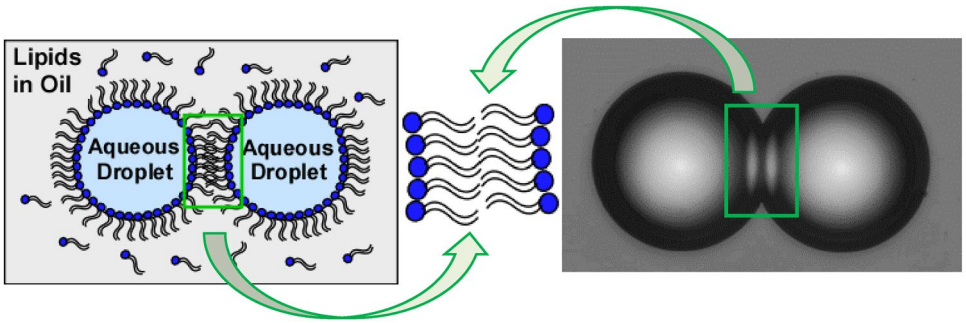

Fig. 1 The droplet interface bilayer (DIB) is formed by contacting apposed monolayers to form a bilayer when aqueous droplets are brought together in an immiscible oil medium, forming a structure simulating the cell membranes consisting of a double leaflet of lipids organized into a lipid bilayer structure. The droplets are shown in the photomicrograph are ca. 100 μm in diameter

of lipidic amphiphiles at the interdroplet interface serves to provide flexible levers for probing structural effects (Foley et al. 2020; Lee 2018; Lopez et al. 2018, 2017), including exploration of the effects of exogenous molecules on membrane properties (Wood et al. 2021).

By building upon the foregoing, this work aims to (1) investigate the ability of RSV to tune the dynamic properties of lipid membranes based on a platform that uses water permeability parameters to probe lipid bilayer structural modulation, (2) study the interplay of Chol and RSV by assembling Chol-free and Chol-enriched model membranes, and (3) examine these systems with diverse techniques for thermal and structural properties. To the best of our knowledge, there have been no reported studies of how the interaction of RSV with lipid membranes would influence water permeability of the lipid membrane. While a wide range of techniques have been previously used to attain mechanistic insight into the impact of RSV molecules on the lipid bilayer and its influence on its biophysical properties, they often include contradictory findings, and so hence this impact still requires further elaboration. For example, RSV has been reported to either fluidize or, contrarily, rigidify membranes as a result of interactions with the hydrophobic chain region or, the hydrophilic headgroup region of membranes (Brittes et al. 2010; de Ghellinck et al. 2015; Fabris et al. 2008; Han et al. 2017; Ingólfsson et al. 2014; Neves et al. 2015; Tsuchiya et al. 2002; Wesołowska et al. 2009). Additionally, many of the prior studies for assessing the impact of RSV molecules on the bilayer membrane have employed various fluorescent probe molecules which are themselves embedded in the bilayer and can influence bilayer physical properties, and so therefore it is beneficial to elaborate new probe-free methods for investigating RSV effects.

Figure 2 shows the molecular structures of the compounds employed in the present studies. As the principal component of a DIB model membrane, we used a neutral zwitterionic ester-linked glycerophosphocholine lipid commonly found in eukaryotic cell membranes, namely,

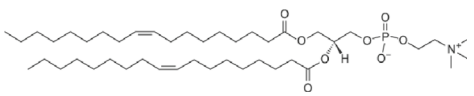

1,2-dioleoyl-*sn*-glycero-3-phosphocholine (18:1 (Δ9 cis) PC, DOPC)

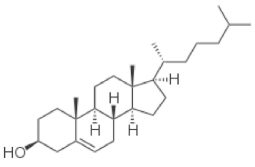

Cholesterol (CHOL)

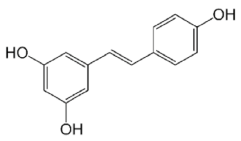

trans-Resveratrol (RSV)

Fig. 2 Structures of DOPC, cholesterol, and *trans*-Resveratrol molecules

1,2-dioleoyl-*sn*-glycero-3-phosphocholine (DOPC), which comprises a headgroup portion with negatively charged phosphate (PO_4^-) group and a positively charged ammonium ($N(CH_3)_3^+$) group. We also used two different mixtures of DOPC with Chol (4 to 1, and 2 to 1, mole ratio of DOPC to Chol respectively) to represent a membrane providing a more complex biomimetic composition. Cholesterol consists of a rigid tetracyclic ring structure with a hydroxyl group at one end and a short hydrocarbon tail at the other. Resveratrol (RSV), 3,5,4′-trihydroxystilbene, consists of two phenolic rings, one single- and another double-hydroxylated, connected by an ethylene bridge. The *trans*-isoform is the most extensively studied major isoform (Salehi et al. 2018).

Experimental Section

Materials and Sample Preparations

Lipids used in the current study were obtained from Avanti Polar Lipids, Inc. (Alabaster, AL) with 99 + % purity and used as received without further purification. DOPC was provided as a solution in chloroform. Squalene (2,6,10,15,19,23-hexamethyl-2,6,10,14,18,22-tetracosahexaene; $C_{30}H_{50}$; "SqE") was used as the immiscible organic phase. All other chemicals, including cholesterol (Chol) and *trans*-resveratrol (≥ 99% by HPLC), were of the highest purity available, and were purchased from Sigma-Aldrich and used without additional purification. SqE is chosen as immiscible solvent since it possesses a property of being excluded from the droplet interface bilayer due to its large molecular size, providing essentially solvent-free DIBs (White 1977, 1978). All lipids, Chol, and RSV were stored at -20 ℃ until use and freshly prepared immediately before use in experiments. Precautions to avoid photo-oxidation were taken during preparation of any samples that included RSV or DOPC, and extended light exposure was avoided by wrapping all sample containers with aluminum foil. Solutions containing RSV or DOPC were prepared immediately prior to the experiment in which they were used, and repeated experiments were performed with a new set of samples prepared on each day. SqE was stored in the temperature range of 2 °C – 8 °C. In order to prepare an SqE solution containing DOPC (with or without Chol and RSV), the chloroform solution of DOPC (optionally with Chol) is evaporated under inert gas to make a dried thin film of lipid or lipid mixture, followed by overnight vacuum drying for complete removal of any residual solvent. When RSV is used, it is co-dissolved with the lipid or lipid mixture. The appropriate amount of RSV (stock solution is prepared using chloroform/methanol (8/2, v/v) as solvents for RSV) is co-dissolved with lipid (or lipid mixture with Chol) in chloroform, followed by the complete evaporation of the solvent

to generate a dried RSV/lipid film of defined mole ratio. For water permeability experiments, this dried RSV/lipid film is then dissolved in SqE, to a total lipid concentration of 5 mg/mL. When Chol is present, it is included in a mole ratio of DOPC to Chol of 4:1 or 2:1. In some experiments, RSV is employed as a freshly prepared aqueous solution (n.b.; the water solubility of RSV is ca.0.003 g/100 mL at 25 ℃), as described more fully in the result section. For sample preparations used in Differential Scanning Calorimetry (DSC), dried RSV/lipid films described above are subsequently rehydrated with pure water, to a total lipid concentration of ~ 16 mg/mL and vortexed vigorously for about 5 min to obtain a suspension of multilamellar vesicles (MLVs), followed by bath sonication of ca. 30 min. For sample used in confocal Raman microspectroscopy, a suspension of MLVs prepared above are further treated with seven freeze–thaw cycles using liquid nitrogen. Aqueous solutions containing osmolytes (NaCl at nominally 0.1 M) were prepared from deionized water (18.2 MΩ·cm) purified in a Millipore water purification system (Direct Q-3). No pH control was performed. The osmolality (in mOsm/kg) of all aqueous solutions used was measured by a vapor pressure osmometer (VAPRO model 5600) immediately after fresh preparation of each solution, as well as prior to use.

Water Permeability Measurement using Droplet Interface Bilayer (DIB) as Model Biological Membrane

The water permeability measurement was performed using the model membrane formed by the DIB method. A similar set-up has been used as previous papers from our research group and the detailed experimental set-up and methodology are described in the supplemental information. As shown in Fig. 3, the system consistsof an inverted microscope with two micropipet manipulators. When two osmotically imbalanced droplets, each covered with a monolayer (one being a pure water, and the other being a droplet of 0.1 M NaCl) are brought together to form a bilayer, water transport begins immediately, resulting in swelling droplet and shrinking droplet. The respective time changes in droplet volume are optically measured by microscopic observation. All water permeability experiments in this study were carried out at 30 °C.

Differential Scanning Calorimetry

Thermal phase transition study was performed on a TA Q2000 Differential Scanning Calorimeter (DSC) and analyzed using TA Universal Analysis software for the main phase transition behavior of the samples. The main phase transition temperature, T_m, corresponds to the temperature at the apex of the endothermic transition peak. The phase

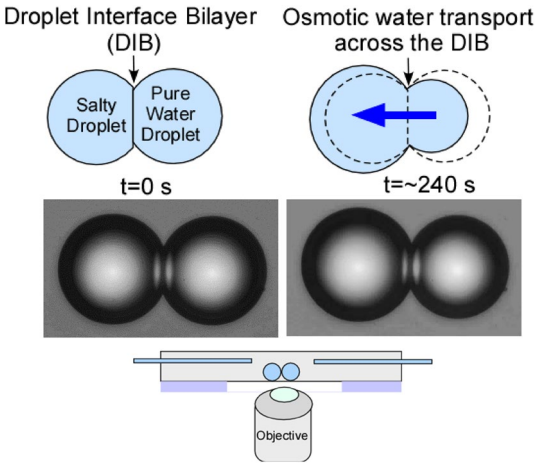

Fig. 3 Schematics of the experimental set-up showing two aqueous microdroplets in a hydrocarbon dispersion of DOPC (or DOPC with Chol) using SqE solvent. When an imbalance in osmotic pressure is present between two aqueous droplets that adhere at a droplet interface bilayer, subsequent osmotic water transport is monitored and recorded for ~ 5 min (arrow: the direction of water transport), as shown in representative videomicrographs of progression of typical DIB permeability experiment. The starting size of each aqueous microdroplet is typically in ~ 100 μm diameter

transition enthalpy was obtained by integrating the area under the heat capacity curve. About 15 μL of the MLVs prepared described above was hermetically sealed and heated and cooled at rates of 5 ℃/min. The following temperature program is used for the DSC experiment for each sample: equilibrate at -40 °C; heating ramp from -40 °C to 0 °C at 5 °C/min; isothermal at 0 °C for 0.5 min; cooling ramp from 0 °C to -40 °C at 5 °C/min; heating ramp from -40 °C to 0 °C at 5 °C/min, under high purity nitrogen with a flow rate of 50 ml/min. Reported values are determined from two to three different samples. Each sample was cycled three times to check if there is any hysteresis and in all cases, reproducible results were obtained on consecutive heating and cooling cycles. We did not observe any hysteresis.

Confocal Raman Microscpectroscopy

The Raman spectra for supported DOPC bilayers with incorporated RSV, were obtained using a confocal Horiba XploRA INV (Nikon Eclipse Ti-U) equipped with an internal air-cooled solid-state laser at 532 nm and a thermoelectrically cooled CCD detector. The samples (10 – 20 μL), acquired immediately from a freeze–thaw process (see sample preparation c section), were spread on glass coverslips (#1.5), previously cleaned with ethanol and dried with nitrogen. The film of solid supported bilayers on hydrophilic surface was attained after removing residual aqueous solvent by placing the coverslips on a heating plate held at ~ 30 °C in a closed home-made chamber. Accumulated spectra were

acquired with 40 X microscope objective (N.A.0.60) and a grating of 1200 lines per millimeter. All Raman spectra described herein are obtained at ambient room temperature, ~25 °C.

Results and Discussion

Effects of Resveratrol (RSV) on Water Permeability

Figure 4 and Table 1 display the osmotic water permeability coefficients (P_f) of DOPC-based membranes at 30 °C as a function of varying mole fraction of RSV in the DOPC-RSV mix. As shown schematically in Fig. 4, RSV is present in an appropriate mole ratio with DOPC in SqE. The results in Fig. 4 indicate that P_f for water transport *decreases* with increasing concentration of RSV. When compared to that of DIB formed from pure DOPC as a control, there was an approximately 5% decrease in water permeability, from 74 ± 4 to 70 ± 4 µm/s, in the presence of 100:1 DOPC to RSV mole ratio. The decrease in water permeability is further enhanced with increasing concentration of RSV, reaching 59 ± 4 µm/s at 4:1 DOPC to RSV mole ratio, which is a decrease of about 20% from the P_f of the DIB formed from pure DOPC at the same temperature.

Alternative water permeability experiments were also run, in which the RSV is introduced in aqueous solution in a pair of osmotically unbalanced aqueous droplets, one droplet containing solely RSV, and the other droplet containing 0.1 M NaCl with an identical concentration of RSV (Fig. 5). One can roughly provide an estimate of the ratio of RSV molecules to lipid molecules, for the case of RSV dissolved in the aqueous compartment of an aqueous microdroplet which is coated with a lipid monolayer. For an aqueous droplet of nominal diameter of 100 µm containing 130 µM RSV, where the surface of the droplet is coated with phospholipid (area per lipid, ca. 70 Å^2), there is approximately an equimolar quantity of RSV to lipid (1.09:1 lipid:RSV). Thus, the experiment in which the bilayer is presented with RSV via aqueous solution, is roughly comparable in order of magnitude of the respective components to the case where both RSV and lipid are in the oil phase originally.

Owing to the very poor water solubility of RSV in water, the maximum aqueous concentration of RSV solution that can be prepared is 130 µM (solubility in water: 3 mg/100 mL). As seen in Fig. 5, however, the water permeability across DOPC membranes is clearly affected even at an RSV concentration of 13 µM, indicating that low RSV

Table 1 Effect of resveratrol on osmotic water permeability at 30 °C for DOPC membrane

DOPC: Resveratrol mole ratio	P_f (µm/s) Avg ± SD
No RSV (control)	74 ± 4
100:1	70 ± 4**
50:1	64 ± 3**
30:1	63 ± 4*
10:1	62 ± 4**
4:1	59 ± 4**

**$p < 0.01$

*$p < 0.05$

P values were calculated for each successive concentration of RSV versus immediately prior concentration. *P* values < 0.05 were considered statistically significant

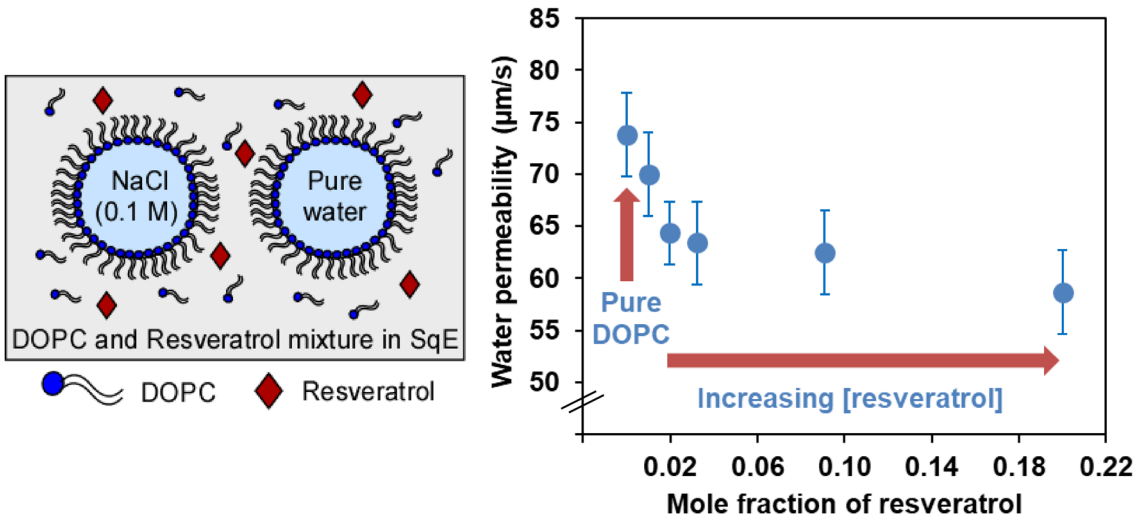

Fig. 4 Osmotic water permeability coefficients (µm/s) of lipid bilayer formed from DOPC at 30 °Cwith varying mole fraction of RSV. RSV is present in an appropriate mole ratio with DOPC in SqE. Each data point represents an average of individual permeability runs (n ≥ 50), and standard deviation as error bars

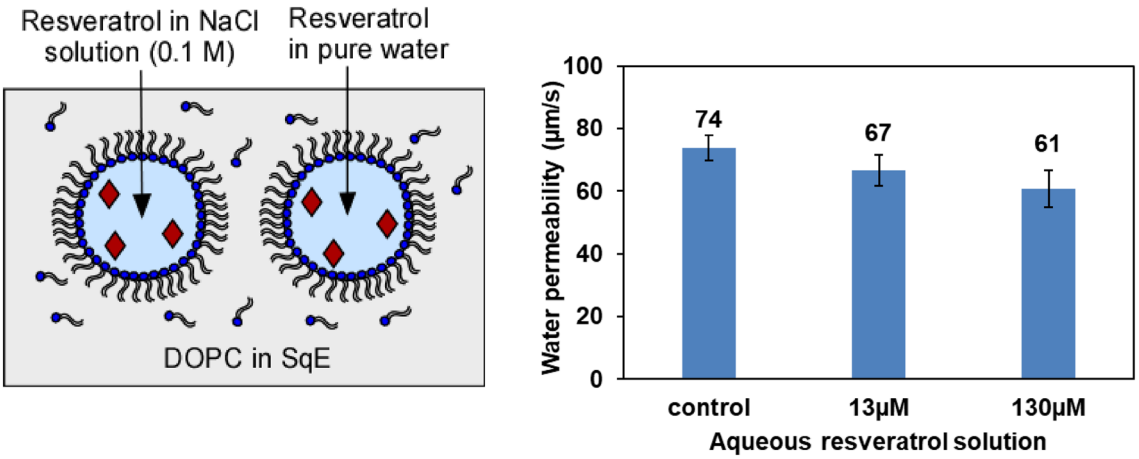

Fig. 5 Osmotic water permeability coefficients (μm/s) of lipid bilayer formed from DOPC at 30 ℃ with varying concentrations of RSV in aqueous droplet. Each data point represents an average of individual permeability runs (n ≥ 30), and standard deviation as error bars

concentration has an impact on the barrier properties of the membranes. Both Figs. 4 and 5 shows the ability of resveratrol *reducing* the water permeabilities of DOPC membrane, regardless of different experimental approaches to introduce RSV molecules into the model membrane.

We further incorporated Chol into the DOPC bilayer to determine the effect of RSV upon the water permeability of the Chol-enriched bilayer. Increasing amounts of Chol in DOPC membranes have been reported to cause a corresponding decrease in the area occupied by the lipid and also correspond to a decrease in the water permeability across these membranes (Mathai et al. 2008). The condensing effect of Chol in DOPC lipid bilayers, as studied via atomistic MD simulation, revealed that mixtures of DOPC − Chol do not exhibit phase separation at Chol mole fractions of 0.25 and 0.5 (Jurak and Chibowski 2015). For DOPC-Chol mixtures, the surface area per lipid ratio has a near-linear decrement with increasing Chol concentrations (Boughter et al. 2016). As shown in Fig. 6, the water permeabilities of the DOPC lipid bilayer made of 4:1 and 2:1 mol ratios of DOPC:Chol (without RSV) is 70 ± 3 μm/s and 68 ± 3 μm/s, respectively, compared to 74 ± 4 μm/s for pure DOPC at 30 °C; these results are consistent with literature findings of reduction in water permeability. Figure 6 illustrates the effect of varying levels of RSV on water permeability parameters for Chol-containing bilayers. The bilayers tested were composed of 4:1 and 2:1 mol ratio of DOPC:Chol, and the amount of RSV is denoted in terms of mole ratio of total lipid (DOPC and Chol) to RSV, which was in the range from 30:1 to 4:1.

As seen in Fig. 6 and Table 2, with increasing concentration of RSV, there seems to be no significant changes in water permeability of DOPC bilayers containing Chol within the standard deviation. This observation is a contrast to the pure DOPC scenario (in the absence of Chol (blue circles)), where water permeability sharply decreased with increasing

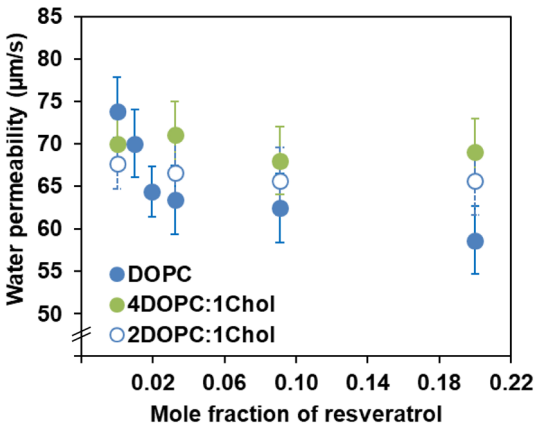

Fig. 6 Osmotic water permeability coefficients (μm/s) of lipid bilayer formed from DOPC with Chol (4:1 and 2:1 mol ratio) at 30 ℃ with varying mole fraction of RSV. P_f for pure DOPC is also shown, for comparison (filled blue circle). Each data point represents an average of individual permeability runs (n ≥ 50), and standard deviation as error bars

RSV concentation. It appears that the presence of Chol in DOPC bilayers suppresses the ability of RSV to decrease the water permeability. When compared to the effect of RSV on pure DOPC, it becomes evident that Chol strongly counteracts the membrane stiffening effect of the RSV, resisting overall effects on the membrane barrier properties induced by the RSV. These results may indicate the important role of Chol in the stability of membranes and demonstrate how Chol is able to increase the ability of a membrane to resist global changes in its physical properties.

In general, water permeability has been shown to be dependent on the physical properties of individual lipids and their bilayered aggregates, such as bilayer thickness, membrane fluidity/rigidity, and area per molecule in the array (Mathai et al. 2008; Olbrich et al. 2000). Overall, fluidity/

Table 2 Osmotic water permeability at 30 °C with increased concentration of RSV for DOPC lipid bilayer containing varying amount of CHOL

(DOPC + CHOL):RSV mole ratio	DOPC:CHOL = 4:1 mol P_f (μm/s) Avg ± SD	DOPC:CHOL = 2:1 mol P_f (μm/s) Avg ± SD
No RSV (control)	70 ± 3	68 ± 3
30:1	71 ± 4*	67 ± 4*
10:1	68 ± 4**	66 ± 4*
4:1	69 ± 4*	66 ± 4*

$^{**}p < 0.01$

$^{*}p < 0.05$

P values were calculated for each successive concentration of RSV versus immediately prior concentration. *P* values < 0.05 were considered statistically significant

rigidity in bilayers is generally correlated with packing density of lipids (Stubbs and Smith 1984), and water permeability is indeed expected to depend on the lipid packing in the bilayer region. Our findings demonstrated a differential behavior of water permeability, in which RSV decreased water permeability for DOPC lipid bilayers while having no significant impact for Chol-enriched DOPC bilayers, which are consistent with prior reports of a rigidifying effect for RSV, depending on initial state of bilayer packing and fluidity. For example, Tsuchiya et al. (Tsuchiya et al. 2002) reported that RSV rigidified the hydrophobic regions of membrane lipid bilayers using fluorescence polarization of unsaturated liposomal membranes, and that the membrane rigidifying effectiveness decreases with higher concentrations of Chol. Neutron reflectometry was used by de Ghellinck et al. (2015) to investigate solid supported DPPC or DPPC/Chol bilayers in their fluid state (at 335 K), and they reported that RSV accumulates between the PC lipid headgroups, causing conformational changes in the tilt angle of the lipid headgroups to a more upright orientation, leading to a reduction of the area per headgroup, and increase of the average thickness of the headgroup layer. However, when both Chol and RSV are present, the ordering effect of Chol on the hydrophobic core is reported to be absent. Han et al. (Han et al. 2017) studied the influence of RSV on the membrane fluidity and polarity of liposomes using membrane-binding fluorescent probes, and reported that the membrane fluidity significantly decreased after the addition of RSV to disordered DOPC liposomes, although it had little effect on more ordered liposomes containing DOPC/sphingomyelin/Chol and sphingomyelin/Chol. Neves et al. (Neves et al. 2016a) reported that the presence of RSV is shown to stiffen the DMPC membrane in the liquid-crystalline phase, while the opposite effect is seen when DMPC is in the gel phase. There is an apparently greater affinity of RSV for the fluidic membrane (egg-PC) (resulting in increase of microviscosity and stiffness of bilayer), than for the tightly packed membrane models (egg-PC containing Chol and sphingomyelin) (Neves et al. 2015). It has also been reported that RSV stabilizes the formation of liquid-ordered domains in liposomes made of egg-PC, Chol, and sphingomyelin, and confers structural organization and order to the membranes (Neves et al. 2016b, 2016c). Studies by Balanc et al. (Balanč et al. 2015) indicate that RSV is incorporated in the inner part of the liposome membrane of PC mixtures leading to reduction in membrane fluidity, as revealed by EPR and fluorimetry. Furthermore, it has been reported that the affinity of DPPC membranes for RSV is greatly decreased in the presence of Chol (Collado et al. 2016). The foregoing are in contrast to some previous reports describing an ability of RSV to disorder membranes and increase fluidity (Brittes et al. 2010; Fei et al. 2018; Olas and Holmsen 2012).

The greater extent of decrease in water permeability of pure DOPC membranes relative to Chol-containing membranes may be related to both the relatively large molecular area (71 $Å^2$) of DOPC and a high degree of fluidity of the membrane relative to the Chol-containing case, thereby readily allowing for the penetration of RSV into the membrane. Additionally, membrane binding of RSV has been reported to lead to an increased dehydration of the headgroups, as a result of the affinity of hydroxyl groups in RSV to water molecules, thus altering the polar environment of the liposome membrane, and cascading from a "disordered" membrane to an "ordered" one (Han et al. 2017). This behavior may also contribute to our observed decrease in water permeability.

Effects of RSV on Thermotropic Properties

The endothermic DSC thermograms for DOPC MLVs in the presence of different concentrations of RSV is shown in Fig. 7 along with the corresponding thermodynamic data in Table 3. The thermogram of DOPC MLVs in the absence of RSV (Fig. 7, control) shows well-defined endothermic transitions, arising from the transition of the lamellar gel phase L_β to the lamellar liquid-crystalline state L_α at the temperature $T_m = -16.8$ °C with an enthalpy of 10.34 kcal/mol, which is in agreement with literature data ($T_m = -18.3 \pm 3.6$ °C, $\Delta H = 9.0 \pm 2.8$ kcal/mol) (Koynova and Caffrey 1998). The low T_m indicates that DOPC membrane is in the disordered

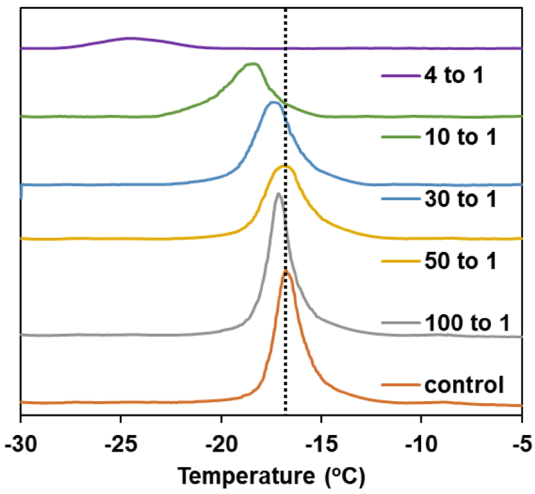

Fig. 7 Endothermic calorimetric thermograms of DOPC MLVs containing different concentrations of RSV; from bottom to top in mole ratio DOPC to RSV: (control) pure DOPC, 100 to 1, 50 to 1, 30 to 1, 10 to 1, and 4 to 1. The vertical dotted line represents the T_m for pure DOPC

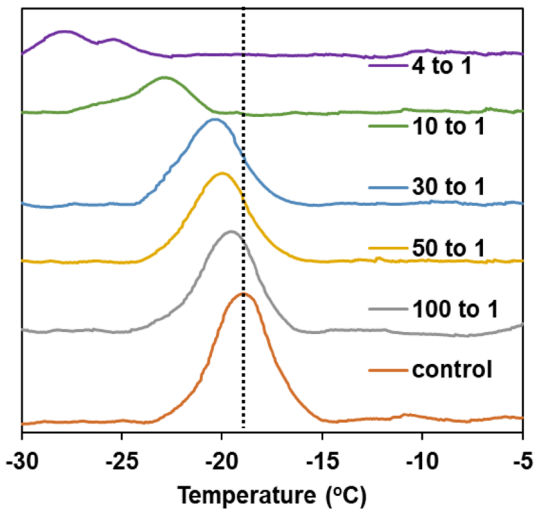

Fig. 8 Endothermic calorimetric thermograms of DOPC:Chol (4 to 1 mol ratio) MLVs containing different concentrations of RSV; from bottom to top, the mole ratio of total lipid (DOPC:Chol) to RSV was 100 to 1, 50 to 1, 30 to 1, 10 to 1, and 4 to 1, respectively. The dotted line represents the T_m for pure DOPC:Chol (4:1 mol ratio) for comparison

Table 3 Thermodynamic parameters (T_m and ΔH) for main phase transition of DOPC MLVs at different concentrations of RSV

Lipid to RSV (mol)	DOPC MLVs	
	T_m (°C)	ΔH (kcal/mol)
Control	− 16.8	10.34 ± 0.25
100 to 1	− 17.1	10.33 ± 0.30
50 to 1	− 16.8	8.35 ± 0.40
30 to 1	− 17.5	9.42 ± 0.30
10 to 1	− 18.4	8.07 ± 0.25
4 to 1	− 24.5	2.77 ± 0.30

Table 4 Temperature (T_m) and enthalpy (multilamellar liposome ΔH), for main phase transition of DOPC:Chol (4 to 1 mol ratio) MLVs at varying concentrations of RSV

Total lipid (including both DOPC and Chol) to RSV (mol)	DOPC:Chol (4:1 mol) MLVs	
	T_m (°C)	ΔH (kcal/mol)
Control	− 18.9	4.09 ± 0.28
100 to 1	− 19.5	3.32 ± 0.10
50 to 1	− 20.0	2.88 ± 0.10
30 to 1	− 20.4	2.96 ± 0.15
10 to 1	− 22.8*	1.46 ± 0.14*
4 to 1	− 27.9*	0.89 ± 0.25*

*Represent the T_m for the highest endothermic transition peak. Enthalpy data represents the total area for all peaks

fluidic state, a condition usually associated with the presence of unsaturated acyl chains. Figure 7 and Table 3 show that the main phase transition of the DOPC is affected by RSV as a function of RSV concentration, leading to a shifting toward lower T_m temperature and an overall broadening, which effects are more marked at relatively higher RSV concentrations. When RSV in included in the bilayer at 100:1 mol ratio of DOPC to RSV, T_m is decreased by 0.3 °C compared to pure DOPC, with no measurable changes in ΔH. These values gradually changed with increasing mole ratios of RSV. At 4 to 1 mol ratio, the peak is significantly suppressed, as evidenced by a reduction of its enthalpy from 10.34 kcal/mol (pure DOPC) to 2.77 kcal/mol, and the main transition is shifted to a lower temperature by 7.7 °C (from − 16.8 °C to − 24.5 °C). However, no further reduction in T_m and ΔH are seen for 2 to 1 and 1 to 1 mol ratio (data not shown), hinting that there may be a saturation at and above RSV mole ratio content of 4 to 1 (DOPC to RSV).

Additional DSC experiments were performed in the lower concentration ranges of 1500 to 1, 600 to 1, and 150 to 1 (results shown in supplemental data Figure S2), and a negligible shift of ΔT_m to lower temperature (ca. < 0.1 °C) is observed, with no changes in ΔH value.

The DSC thermograms for the DOPC/Chol (4 to 1 mol ratio) lipid bilayers, as a function of increasing RSV concentration, are shown in Fig. 8 and Table 4. In the absence of RSV, the addition of Chol significantly changes the thermotropic properties of pure DOPC (Fig. 8, control). The main transition is shifted to a lower temperature (from − 16.8 °C for pure DOPC to − 18.9 °C for 4DOPC/1Chol), and the peak is significantly suppressed (from 10.34 kcal/mol for pure DOPC to 4.09 kcal/mol for DOPC/CHOL at 4 to 1 mol

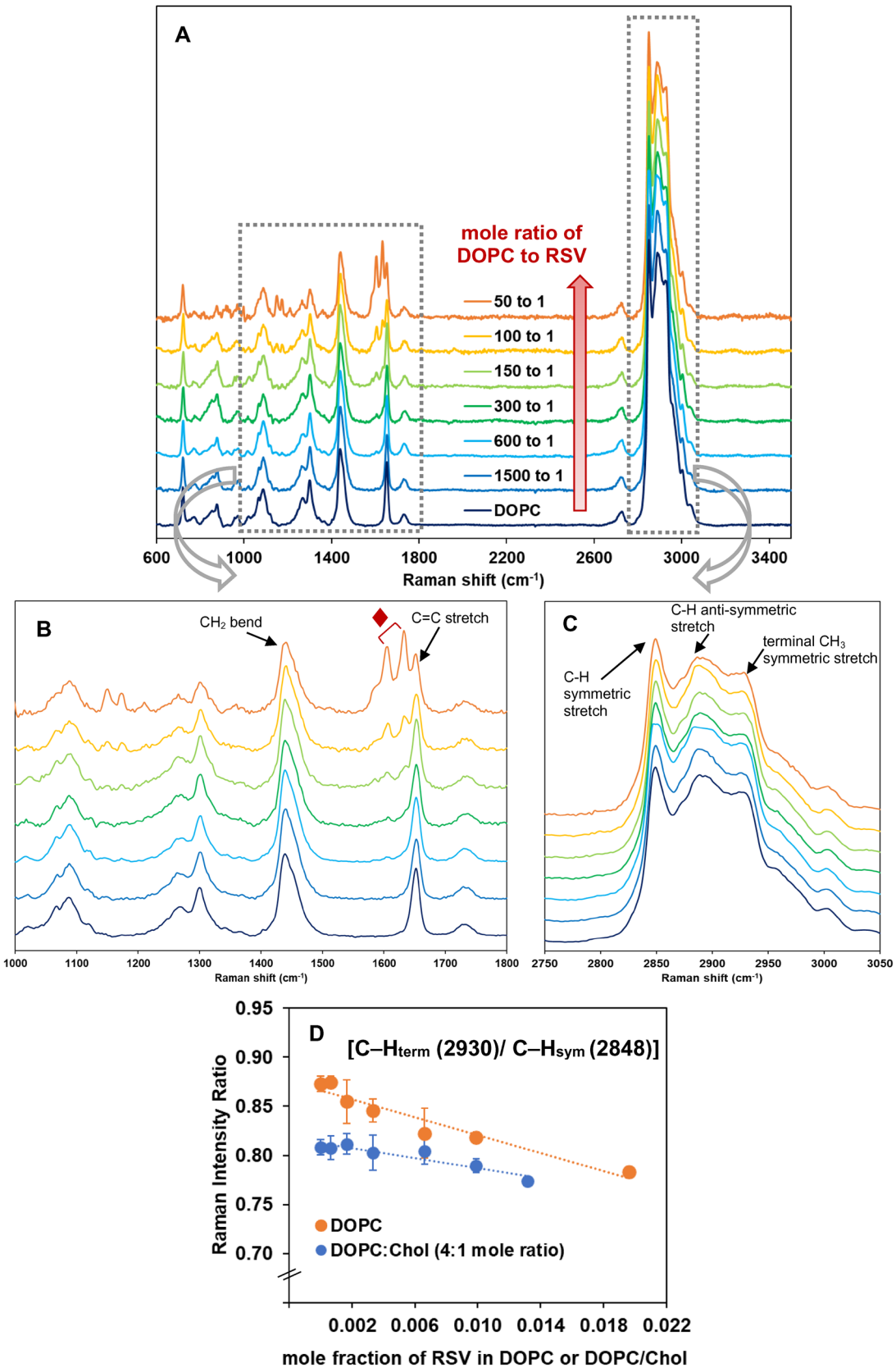
A
mole ratio of DOPC to RSV
50 to 1
100 to 1
150 to 1
300 to 1
600 to 1
1500 to 1
DOPC
600 1000 1400 1800 2200 2600 3000 3400
Raman shift (cm-1)
B
CH2 bend
C=C stretch
1000 1100 1200 1300 1400 1500 1600 1700 1800
Raman shift (cm-1)
C
C-H anti-symmetric stretch
terminal CH3 symmetric stretch
C-H symmetric stretch
2750 2800 2850 2900 2950 3000 3050
Raman shift (cm-1)
D
[C–Hterm (2930)/ C–Hsym (2848)]
Raman Intensity Ratio
0.95 0.90 0.85 0.80 0.75 0.70
DOPC
DOPC:Chol (4:1 mole ratio)
0.002 0.006 0.010 0.014 0.018 0.022
mole fraction of RSV in DOPC or DOPC/Chol

◂**Fig. 9** **A** Raman spectra of DOPC at various RSV concentrations at ambient temperature, **B** fingerprint region, **C** stretching CH band region. Spectra are vertically shifted for clarity. The red diamond region contains two most intense characteristic RSV peaks. Selected peak assignments originated from DOPC is shown. **D** Raman intensity ratios of [$C-H_{term}$ (2930)/$C-H_{sym}$ (2848)] as a function of RSV concentration in DOPC and DOPC/Chol bilayer films. Each data point represents average and standard deviation (SD) derived from 5 to 10 independently prepared samples and each sample is scanned across three different sample regions

ratio). The transition enthalpy is almost abolished at mole ratio 2:1 of DOPC to Chol, with no well-defined enthalpic transition being apparent (data not shown). These results are consistent with many previous reports on DOPC bilayers as a function of cholesterol content (Davis and Keough 1983; Fritzsching et al. 2013). For studies of RSV with Chol-containing bilayers, only the mole ratio of 4 DOPC to 1 Chol was used; higher quantities of Chol would excessively suppress the DSC peak. In general, as the mole fraction of RSV in DOPC/Chol increases, the main transition peak is moved toward lower temperature (Fig. 8 and Table 4). Starting at 30:1 mol ratio of total lipid (DOPC/Chol):RSV, a lower temperature shoulder was observed, presumably due to a phase separation. This became more pronounced at 10:1 total lipid:RSV, seen in the splitting of the peak into two components. The apparent phase separation became more evident at a 4 to 1 mol ratio, with the dominant peak at lower temperature. The enthalpy of transition gradually decreases upon interaction with the RSV from a value of 4.09 kcal/mol in the absence of RSV, to 1.46 kcal/mol at the DOPC/Chol to RSV at 10 to 1 mol ratio, a decrease of about 65%. This is in contrast to the Chol-free DOPC-RSV interaction, where relatively modest enthalpy changes have been seen; for example, at the same RSV concentrations (10 to 1 mol ratio of DOPC to RSV), a decrease in enthalpy of about 20% was induced. However, at the highest concentrations of RSV we tested, a similar extent of reduction in ΔH is seen both Chol-free (73% reduction) and Chol-enriched (78% reduction) bilayers. As noted, there are differential changes in T_m and ΔH for RSV with DOPC versus DOPC/Chol membranes, respectively, indicative of varying membrane interactions of RSV dependent upon Chol concentation in the membrane, and concentration of RSV.

Overall, our DSC results show that RSV interacted with both Chol-free and Chol-enriched DOPC MLVs to induce changes in the bilayer thermotropic properties and influence the conformational configuration of lipid hydrocarbon chains, in a concentration-dependent manner. The progressive decrease in T_m upon inclusion of RSV may reflect stabilization of the fluid phase of the DOPC and/or destabilization of the low-temperature gel phase, which for the fluid phase would indicate molecular disordering.These findings are qualitatively consistent with previous DSC studies, albeit for saturated PCs (Balanč et al. 2015; Fabris et al. 2008; Fei et al. 2018; Koukoulitsa et al. 2011; Longo et al. 2016; Sarpietro et al. 2007; Wesołowska et al. 2009). These prior studies demonstrate that the presence of RSV results in the broadening of the DSC phase transition, reducing the T_m in the DMPC and DPPC multilamellar vesicles in a concentration-dependent manner, with more marked ΔH reduction at higher RSV concentrations. In our unsaturated vesicles, relatively less change in ΔH was observed at the lower limit of RSV concentration in Chol-free DOPC MLVs. Namely, the enthalpy was only slightly lowered from 10.34 kcal/mol (no RSV) to 9.42 kcal/mol at 30 to 1 mol ratio of DOPC to RSV. These data are consistent with previously- posited general findings that molecules inserted into a lipid bilayer array as interstitial impurities (rather than subsituting for lipid) will generally not affect enthalpic changes for the array even as they cause changes in T_m (Jørgensen et al. 1991). Hence, at low concentrations of RSV, it is likely that RSV positions itself at or near the headgroup region of the lipid bilayer, while at high RSV concentrations, an increased interaction with the hydrocarbon chain is more likely as more RSV penetrates into the acyl chain region, which is reflected in greater reduction of ΔH. In addition, the evidence of phase separation induced by RSV at high concentration (i.e., RSV content greater than 10:1 total lipid:RSV) is more prominent in the Chol-enriched DOPC system, compared to Chol-free DOPC system. In the literature, a similar phase separation has been reported, from a DSC study of DMPC multilamellar vesicles, albeit at higher concentrations of RSV. The two peaks were interpreted as one peak component being associated with the phase transition of RSV-rich lipid domains and another component representing RSV-poor regions (Sarpietro et al. 2007; Wesołowska et al. 2009). A synchrotron X-ray scattering study of lipid bilayers also shows that RSV induces phase separation of egg-PC (EPC) bilayers, which has been interpreted as being a result of favorable van der Waals interactions between phenol rings of RSV and the hydrocarbon chain of lipid (Neves et al. 2016b). Additional studies using Förster resonance energy transfer and DPH fluorescence quenching assays reported a phase separation and domain formation induced by RSV in bilayers of EPC, EPC:Chol, and EPC:Chol:SM (Neves et al. 2016c).

Effects of Resveratrol on Structural Properties of Lipid Arrays

We have employed confocal Raman microspectrosopy of supported lipid bilayers to monitor changes upon interaction with RSV molecules. Figure 9A shows ambient temperature Raman spectra in the frequency region of $600-3500\ cm^{-1}$ for DOPC supported bilayers containing varying concentrations of RSV. All spectra are normalized to the intensity at $2849\ cm^{-1}$ for comparison. Figure 9B shows characteristic

vibration bands of DOPC bilayers, including CH_2 bend (~ 1440 cm^{-1}) and C = C stretching (~ 1650 cm^{-1}). The fingerprint region also contains the most intense characteristic Raman bands from RSV, 1606 and 1632 cm^{-1}, which are attributed to a combination of ν(C = C) and δ(C–H) vibrations of the *trans*-olefin carbons together with ν(C = C) vibrations of the phenyl rings (Billes et al. 2007; Vongsvivut et al. 2008). An additional set of assignments of characteristic Raman peaks for pure DOPC and RSV is shown in Supporting Information (Table S1). Increased content of RSV in DOPC membranes is reflected in the increasing intensity of the peaks at 1606 and 1632 cm^{-1}. Figure 9C shows the C – H stretching region (2750 – 3050 cm^{-1}), a portion of the spectrum which exhibits strong Raman scattering for phospholipid molecules. It is the most well-studied region of the lipid membrane spectrum for its correlations to hydrocarbon chain order (Levin and Lewis 1990). Peaks centered at approximately 2850 and 2890 cm^{-1} are assigned to the methylene C – H symmetric ("C – H_{sym}") and C – H anti-symmetric stretching modes, respectively. The peak at ~ 2930 cm^{-1} is assigned to the symmetric stretching mode for the hydrocarbon chain terminal methyl C – H, "C – H_{term}" (Fox et al. 2007; Orendorff et al. 2002). Importantly, the C – H stretching region (2750 – 3050 cm^{-1}) has no peaks from RSV that interfere with peaks from DOPC. Much prior work has been performed establishing that these three foregoing peaks in the C – H stretching region, and their ratios *vis-a-vis* each other, are useful indicators for determining membrane structural properties (Fox et al. 2006, 2007; Orendorff et al. 2002). Therefore, the spectral differences in this region were used to identify conformational changes of the DOPC membranes upon interaction with RSV molecules. Specifically, the ratios of peak intensity of [C – H_{term}/C – H_{sym}] is used as a measure of hydrocarbon chain order/disorder and packing. As seen in Fig. 9D, increased concentration of RSV in the DOPC leads to a gradual decrease in the peak intensity ratio of [C – H_{term} (2930)/C – H_{sym} (2848)], which span the range of from 0.87 to 0.78. A *decrease* in the [C – H_{term}/C – H_{sym}] intensity ratio indicates a *decrease* in rotational disorder and freedom of motion of the hydrocarbon chain. Hence the decreasing ratios with increased RSV content appears to indicate that a greater quantity of RSV molecules interacting with a DOPC lipid bilayer affects intermolecular chain coupling in the hydrocarbon chain region, progressively strengthening packing order, thereby having an ordering effect on DOPC lipid bilayers. The Raman mode near 719 cm^{-1} corresponds to C – N symmetric stretching vibrations of the choline $[–N(CH_3)_3]^+$ group and its shift was observed from 719 cm^{-1} for pure DOPC, to 723 cm^{-1} for 600 to 1 and higher content of RSV, which indicates a binding of RSV to the headgroup.

Analogous Raman structural analyses in the C – H stretching region has been extended to DOPC/Chol mixtures. However, this C – H stretching region (2750 – 3050 cm^{-1}) also has peaks stemming from Chol, which interfere with peaks from DOPC. Therefore, peak analysis was performed after subtraction of the Chol-originated peaks from the spectra of the mixture of DOPC and Chol (de Lange et al. 2007; Tantipolphan et al. 2006). The detailed spectral subtraction method is described in the supplemental information (Figure S3). Figure 9D compares the peak intensity ratio of [C – H_{term} (2930)/C – H_{sym} (2848)] as a function of increasing RSV mole fraction in DOPC/Chol bilayers (4 to 1 mol ratio), along with Chol-free DOPC bilayers. Overall, the decrease in the peak ratio is much less pronounced compared to that of pure DOPC bilayers. This is pronounced in the regime of low content of RSV, where there appears to be no significant differences with increasing RSV. A decrease only becomes apparent at the high content of RSV, and even so, the slope of the curve in Fig. 9D for the Chol-containing membrane is less than that of the pure DOPC membrane. RSV induced conformational change of lipids studied by confocal Raman spectroscopy is rare to our knowledge, with an exception of a study of RSV encapsulation in soy-PC liposomes in which lipid chain ordering was detected in the presence of RSV in certain liposome formulation (Tosato et al. 2018). Our findings from these Raman spectroscopic studies are consistent with the decreasing water permeability for increasing in RSV concentrations; the greater the degree of order and increased packing density, the lesser the water permeability. This indicates that packing in the hydrocarbon chain regions of RSV-containing DOPC plays a role in the passive water transport process. Additionally, RSV did not induce any marked hydrocarbon chain ordering effect in the presence of Chol, which is consistent with there being no measureable water permeability changes, as described earlier.

Conclusions

The non-specific interactions between RSV and cell membranes can modulate structural and physical properties of membranes and the resultant perturbations of membrane properties may affect the conformation of proteins inserted within the membrane, disturbing the membrane-hosted biological functions. Hence, an enhanced understanding of the interaction of RSV with the cell membrane at the molecular level plays an essential role in providing insight into improved therapeutic activities. We have examined the interaction of RSV molecules with model bilayer membranes composed of DOPC with varying content of Chol, using a combination of techniques: studies of bilayer water permeability across the DIB to infer modulations in the bilayer physical state; DSC; and confocal Raman microspectroscopy. The combined results from diverse experimental

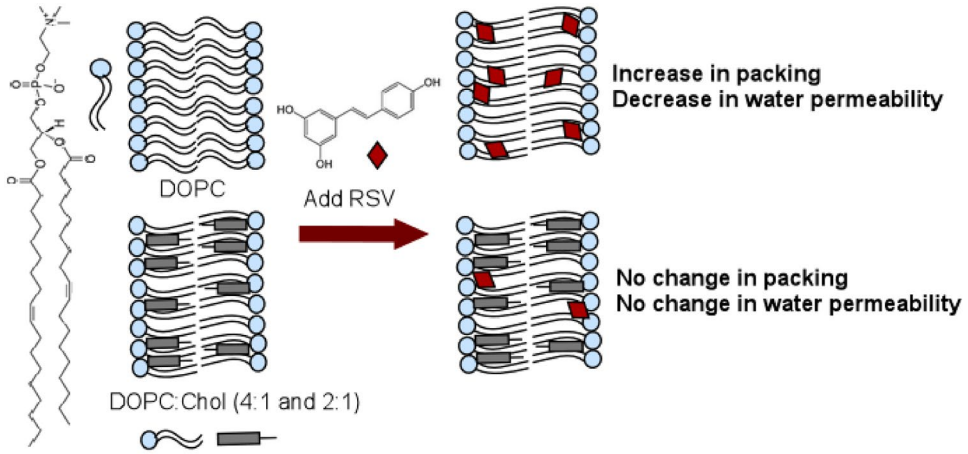

Fig. 10 Schematic representation of RSV interaction with Chol-free and Chol-enriched DOPC lipid bilayer

techniques provide evidence for differential non-specific interaction between RSV and DOPC membranes, relative to Chol-enriched DOPC membranes. The nature and extent of interactions greatly depend on the presence and absence of Chol as well as the concentration of RSV. This is schematically shown in Fig. 10.

Our results suggest that progressive inclusion of RSV in the DOPC membranes results in reduction of the osmotic water permeability. We take this as an indication that there is a capability of RSV to stiffen fluidic membranes, driven by hydrogen-bonding interactions of RSV hydroxyl groups with polar lipid headgroup and hydrophobic interactions between phenyl ring of RSV with hydrocarbon chain. However, in the presence of Chol in the DOPC membrane, there is little change in water permeability; it would appear that the Chol-containing membranes, having a higher hydrocarbon chain order, exhibit little or no change in their water transport parameters regardless of the presence of RSV. One possible reason why RSV is not able to decrease P_f in DOPC/Chol membranes to the same ultimate value as in pure DOPC, is that Chol may inhibit the partitioning of RSV to the degree existing for pure DOPC membranes, presumably due to a paucity of free volume in the Chol system. The partition coefficients in our systems were not measured, although the literature does provide effective methodolgies for doing so with liposome/water systems via derivative UV–vis spectrophotometry ((Neves et al. 2015). By this method, Neves et al. provide results suggestive of differing partition coefficients (K_p) for trans-resveratrol in LUVs of egg phosphatidylcholine (EPC) (value of 3384) versus for EPC/Chol (4/1), the K_p is lowered to1186. Alternatively, RSV could still partition into Chol-containing membranes to the same extent as in Chol-free membranes, if Chol positions largely in the membrane interior (with maximum effect on inhibiting permeability), whereas RSV positions closer to headgroups. Evidence for either mechanism will benefit from measurement of RSV partition coefficients for the respective systems, which will form a feature of our future studies.

DSC thermograms show that RSV interacts with DOPC and DOPC/Chol bilayers and influences their thermotropic phase behavior in a concentration-dependent manner, by decreasing the main phase transition temperature and enthalpy, with a phase separation shown at higher concentrations of RSV, a phenomenon more pronounced when Chol is present. The intensity ratios for peaks in the C – H stretching region from Raman bands demonstrate the RSV effect in ordering of the hydrocarbon chain in DOPC supported bilayers, with the greater extent of ordering in the absence of Chol compared to the Chol-enriched DOPC membranes. While there are contradictory reports about the effect of RSV on lipid bilayer, our findings are aligned with previous reports showing the rigidifying effect of RSV and its sensitivity on composition and physical state of the membrane, as well as the concentration of RSV. These results showing markedly reduced passive water permeability in the presence of RSV also may hold vital significance to the mechanism by which RSV inhibits the effect of reactive oxidative species (ROS). As precursors to the highly reactive hydroxyl radical (•OH), molecules such as hydrogen peroxide and hydroperoxyl radical must gain access to buried unsaturated regions of fatty acyl chains to begin lipid peroxidation, a process which would be inhibited by reduced water permeability, given that water and H_2O_2 have many quite similar physical properties (Li et al. 2000; Möller et al. 2019). All of these phenomena are significant in the context of understanding the nature and extent of non-specific interactions between RSV and cell membranes that may lead to potential application to various cancer cell types which are known to have compositionally different membranes, especially with respect to their content of Chol, compared with those of normal cells.

Supplementary Information The online version contains supplementary material available at https://doi.org/10.1007/s00232-022-00250-0.

Acknowledgements The authors would like to acknowledge the financial support from the National Science Foundation (NSF-CHE-2002900, and NSF-MRI-1427705). EP, AGH, JR are NSF S-STEM scholarship recipients, and grateful for the research support in part through NSF S-STEM program (NSF-DUE-1643737). EP is a Clare Boothe Luce Research Scholar and is grateful for the Henry Luce Foundation for the support in part.

Declarations

Conflict of Interest The authors declare they have no financial interests.

References

Alves AC, Ribeiro D, Nunes C, Reis S (2016) Biophysics in cancer: the relevance of drug-membrane interaction studies. BBA-Biomembranes 1858:2231–2244. https://doi.org/10.1016/j.bbamem.2016.06.025

Andersen OS, Koeppe RE (2007) Bilayer thickness and membrane protein function: an energetic perspective. Annu Rev Biophys Biomol Struct 36:107–130. https://doi.org/10.1146/annurev.biophys.36.040306.132643

Athar M, Back JH, Tang X, Kim KH, Kopelovich L, Bickers DR, Kim AL (2007) Resveratrol: a review of preclinical studies for human cancer prevention. Toxicol Appl Pharmacol 224:274–283. https://doi.org/10.1016/j.taap.2006.12.025

Baell JB (2016) Feeling nature's PAINS: natural products, natural product drugs, and pan assay interference compounds (PAINS). J Nat Prod 79:616–628. https://doi.org/10.1021/acs.jnatprod.5b00947

Balanč BD, Ota A, Djordjević VB, Šentjurc M, Nedović VA, Bugarski BM, Ulrih NP (2015) Resveratrol-loaded liposomes: interaction of resveratrol with phospholipids. Eur J Lipid Sci Technol 117:1615–1626. https://doi.org/10.1002/ejlt.201400481

Baur JA, Sinclair DA (2006) Therapeutic potential of resveratrol: the in vivo evidence. Nat Rev Drug Discov 5:493–506. https://doi.org/10.1038/nrd2060

Berman AY, Motechin RA, Wiesenfeld MY, Holz MK (2017) The therapeutic potential of resveratrol: a review of clinical trials. NPJ Precis. Oncol. 1:1–9. https://doi.org/10.1038/s41698-017-0038-6

Billes F, Mohammed-Ziegler I, Mikosch H, Tyihák E (2007) Vibrational spectroscopy of resveratrol. Spectrochim Acta A Mol Biomol 68:669–679. https://doi.org/10.1016/j.saa.2006.12.045

Boughter CT, Monje-Galvan V, Im W, Klauda JB (2016) Influence of cholesterol on phospholipid bilayer structure and dynamics. J Phys Chem B 120:11761–11772. https://doi.org/10.1021/acs.jpcb.6b08574

Brittes J, Lucio M, Nunes C, Lima J, Reis y, (2010) Effects of resveratrol on membrane biophysical properties: relevance for its pharmacological effects. Chem Phys Lipids 163:747–754. https://doi.org/10.1016/j.chemphyslip.2010.07.004

Brown DA, London E (2000) Structure and function of sphingolipid- and cholesterol-rich membrane rafts. J Biol Chem 275:17221–17224. https://doi.org/10.1074/jbc.R000005200

Colin D, Limagne E, Jeanningros S, Jacquel A, Lizard G, Athias A, Gambert P, Hichami A, Latruffe N, Solary E, Delmas D (2011) Endocytosis of resveratrol via lipid rafts and activation of downstream signaling pathways in cancer cells. Cancer Prev Res 4:1095–1106. https://doi.org/10.1158/1940-6207.capr-10-0274

Collado AdAM, Dupuy FG, Morero RD, Minahk C (2016) Cholesterol induces surface localization of polyphenols in model membranes thus enhancing vesicle stability against lysozyme, but reduces protection of distant double bonds from reactive-oxygen species. BBA-Biomembranes 1858:1479–1487. https://doi.org/10.1016/j.bbamem.2016.04.002

Crozier A, Jaganath IB, Clifford MN (2009) Dietary phenolics: chemistry, bioavailability and effects on health. Nat Prod Rep 26:1001–1043. https://doi.org/10.1039/b802662a

Davis P, Keough K (1983) Differential scanning calorimetric studies of aqueous dispersions of mixtures of cholesterol with some mixed-acid and single-acid phosphatidylcholines. Biochemistry 22:6334–6340. https://doi.org/10.1021/bi00295a045

de Ghellinck A, Shen C, Fragneto G, Klösgen B (2015) Probing the position of resveratrol in lipid bilayers: a neutron reflectivity study. Colloids Surf b: Biointerfaces 134:65–72. https://doi.org/10.1016/j.colsurfb.2015.06.028

de Lange MJ, Bonn M, Müller M (2007) Direct measurement of phase coexistence in DPPC/cholesterol vesicles using Raman spectroscopy. Chem Phys Lipids 146:76–84. https://doi.org/10.1016/j.chemphyslip.2006.12.007

Delmas D, Aires V, Colin DJ, Limagne E, Scagliarini A, Cotte AK, Ghiringhelli F (2013) Importance of lipid microdomains, rafts, in absorption, delivery, and biological effects of resveratrol. Ann NY Acad Sci 1290:90–97. https://doi.org/10.1111/nyas.12177

Ding X, Zhang W, Li S, Yang H (2019) The role of cholesterol metabolism in cancer. Am J Cancer Res 9:219

Fabris S, Momo F, Ravagnan G, Stevanato R (2008) Antioxidant properties of resveratrol and piceid on lipid peroxidation in micelles and monolamellar liposomes. Biophys Chem 135:76–83. https://doi.org/10.1016/j.bpc.2008.03.005

Fei Q, Kent D, Botello-Smith WM, Nur F, Nur S, Alsamarah A, Chatterjee P, Lambros M, Luo Y (2018) Molecular mechanism of resveratrol's lipid membrane protection. Sci Rep 8:1–12. https://doi.org/10.1038/s41598-017-18943-1

Foley S, Miller E, Braziel S, Lee S (2020) Molecular organization in mixed SOPC and SDPC model membranes: water permeability studies of polyunsaturated lipid bilayers. BBA-Biomembranes 1862:183365. https://doi.org/10.1016/j.bbamem.2020.183365

Fox CB, Horton RA, Harris JM (2006) Detection of drug−membrane interactions in individual phospholipid vesicles by confocal Raman microscopy. Anal Chem 78:4918–4924. https://doi.org/10.1021/ac0605290

Fox CB, Uibel RH, Harris JM (2007) Detecting phase transitions in phosphatidylcholine vesicles by Raman microscopy and self-modeling curve resolution. J Phys Chem B 111:11428–11436. https://doi.org/10.1021/jp0735886

Fritzsching KJ, Kim J, Holland GP (2013) Probing lipid–cholesterol interactions in DOPC/eSM/Chol and DOPC/DPPC/Chol model lipid rafts with DSC and 13C solid-state NMR. BBA-Biomembranes 1828:1889–1898. https://doi.org/10.1016/j.bbamem.2013.03.028

Fulda S (2010) Resveratrol and derivatives for the prevention and treatment of cancer. Drug Discov Today 15:757–765. https://doi.org/10.1016/j.drudis.2010.07.005

Funakoshi K, Suzuki H, Takeuchi S (2006) Lipid bilayer formation by contacting monolayers in a microfluidic device for membrane protein analysis. Anal Chem 78:8169–8174. https://doi.org/10.1021/ac0613479

García-García J, Micol V, de Godos A, Gómez-Fernández JC (1999) The cancer chemopreventive agent resveratrol is incorporated into model membranes and inhibits protein kinase C α activity. Arch Biochem Biophys 372:382–388. https://doi.org/10.1006/abbi.1999.1507

Han J, Suga K, Hayashi K, Okamoto Y, Umakoshi H (2017) Multi-level characterization of the membrane properties of

resveratrol-incorporated liposomes. J Phys Chem B 121:4091–4098. https://doi.org/10.1021/acs.jpcb.7b00368
Harikumar KB, Aggarwal BB (2008) Resveratrol: a multitargeted agent for age-associated chronic diseases. Cell Cycle 7:1020–1035. https://doi.org/10.4161/cc.7.8.5740
Hill WG, Zeidel ML (2000) Reconstituting the barrier properties of a water-tight epithelial membrane by design of leaflet-specific liposomes* 210. J Biol Chem 275:30176–30185. https://doi.org/10.1074/jbc.M003494200
Holden MA, Needham D, Bayley H (2007) Functional bionetworks from nanoliter water droplets. J Am Chem Soc 129:8650–8655. https://doi.org/10.1021/ja072292a
Huang B, Song B-l, Xu C (2020) Cholesterol metabolism in cancer: mechanisms and therapeutic opportunities. Nat Metab 2:132–141. https://doi.org/10.1038/s42255-020-0174-0
Ingólfsson HI, Thakur P, Herold KF, Hobart EA, Ramsey NB, Periole X, De Jong DH, Zwama M, Yilmaz D, Hall K, Maretzky T, Hemmings HC Jr, Blobel C, Marrink SJ, Koçer A, Sack JT, Andersen OS (2014) Phytochemicals perturb membranes and promiscuously alter protein function. ACS Chem Biol 9:1788–1798. https://doi.org/10.1021/cb500086e
Jang M, Cai L, Udeani GO, Slowing KV, Thomas CF, Beecher CW, Fong HH, Farnsworth NR, Kinghorn AD, Mehta RG, Moon RC, Pezzuto JM (1997) Cancer chemopreventive activity of resveratrol, a natural product derived from grapes. Science 275:218–220. https://doi.org/10.1126/science.275.5297.218
Jørgensen K, Ipsen JH, Mouritsen OG, Bennett D, Zuckermann MJ (1991) A general model for the interaction of foreign molecules with lipid membranes: drugs and anaesthetics. BBA-Biomembranes 1062:227–238. https://doi.org/10.1016/0005-2736(91)90397-q
Jurak M, Chibowski E (2015) Characteristics of a phospholipid DOPC/cholesterol bilayer based on surface free energy and its components. RSC Adv 5:66628–66635. https://doi.org/10.1039/C5RA08203J
Keylor MH, Matsuura BS, Stephenson CR (2015) Chemistry and biology of resveratrol-derived natural products. Chem Rev 115:8976–9027. https://doi.org/10.1021/cr500689b
Ko J-H, Sethi G, Um J-Y, Shanmugam MK, Arfuso F, Kumar AP, Bishayee A, Ahn KS (2017) The role of resveratrol in cancer therapy. Int J Mol Sci 18:2589. https://doi.org/10.3390/ijms18122589
Koukoulitsa C, Durdagi S, Siapi E, Villalonga-Barber C, Alexi X, Steele BR, Micha-Screttas M, Alexis MN, Tsantili-Kakoulidou A, Mavromoustakos T (2011) Comparison of thermal effects of stilbenoid analogs in lipid bilayers using differential scanning calorimetry and molecular dynamics: correlation of thermal effects and topographical position with antioxidant activity. Eur Biophys J 40:865–875. https://doi.org/10.1007/s00249-011-0705-4
Koynova R, Caffrey M (1998) Phases and phase transitions of the phosphatidylcholines. BBA-Rev Biomembranes 1376:91–145. https://doi.org/10.1016/S0304-4157(98)00006-9
Kundu JK, Surh Y-J (2008) Cancer chemopreventive and therapeutic potential of resveratrol: mechanistic perspectives. Cancer Lett 269:243–261. https://doi.org/10.1016/j.canlet.2008.03.057
Lee S (2018) Good to the last drop: interfacial droplet chemistry, from crystals to biological membranes. Acc Chem Res 51:2524–2534. https://doi.org/10.1021/acs.accounts.8b00277
Levin IW, Lewis EN (1990) Fourier transform Raman spectroscopy of biological materials. Anal Chem 62:1101A-1111A. https://doi.org/10.1021/ac00220a001
Li Q-T, Yeo MH, Tan BK (2000) Lipid peroxidation in small and large phospholipid unilamellar vesicles induced by water-soluble free radical sources. Biochem Biophys Res Commun 273:72–76. https://doi.org/10.1006/bbrc.2000.2908
Longo E, Ciuchi F, Guzzi R, Rizzuti B, Bartucci R (2016) Resveratrol induces chain interdigitation in DPPC cell membrane model systems. Colloids Surf B Biointerfaces 148:615–621. https://doi.org/10.1016/j.colsurfb.2016.09.040
Lopez M, Evangelista SE, Morales M, Lee S (2017) Enthalpic effects of chain length and unsaturation on water permeability across droplet bilayers of homologous monoglycerides. Langmuir 33:900–912. https://doi.org/10.1021/acs.langmuir.6b03932
Lopez M, Denver J, Evangelista SE, Armetta A, Di Domizio G, Lee S (2018) Effects of acyl chain unsaturation on activation energy of water permeability across droplet bilayers of homologous monoglycerides: role of cholesterol. Langmuir 34:2147–2157. https://doi.org/10.1021/acs.langmuir.7b03590
Lundbæk JA, Collingwood SA, Ingólfsson HI, Kapoor R, Andersen OS (2010) Lipid bilayer regulation of membrane protein function: gramicidin channels as molecular force probes. J R Soc Interface 7:373–395. https://doi.org/10.1098/rsif.2009.0443
Mathai JC, Tristram-Nagle S, Nagle JF, Zeidel ML (2008) Structural determinants of water permeability through the lipid membrane. J Gen Physiol 131:69–76. https://doi.org/10.1085/jgp.200709848
Michalak Z, Muzzio M, Milianta PJ, Giacomini R, Lee S (2013) Effect of monoglyceride structure and cholesterol content on water permeability of the droplet bilayer. Langmuir 29:15919–15925. https://doi.org/10.1021/la4040535
Milianta PJ, Muzzio M, Denver J, Cawley G, Lee S (2015) Water permeability across symmetric and asymmetric droplet interface bilayers: interaction of cholesterol sulfate with DPhPC. Langmuir 31:12187–12196. https://doi.org/10.1021/acs.langmuir.5b02748
Möller MN, Cuevasanta E, Orrico F, Lopez AC, Thomson L, Denicola A (2019) Diffusion and transport of reactive species across cell membranes. In: Trostchansky A, Rubbo H (eds) Bioactive lipids in health and disease. Springer International Publishing, Cham, pp 3–19
Mouritsen OG (2005) Life-as a matter of fat; the emerging science of lipidomics. Springer, New York
Neves AR, Lucio M, Lima JLC, Reis S (2012) Resveratrol in medicinal chemistry: a critical review of its pharmacokinetics, drug-delivery, and membrane interactions. Curr Med Chem 19:1663–1681. https://doi.org/10.2174/092986712799945085
Neves AR, Nunes C, Reis S (2015) New insights on the biophysical interaction of resveratrol with biomembrane models: relevance for its biological effects. J Phys Chem B 119:11664–11672. https://doi.org/10.1021/acs.jpcb.5b05419
Neves AR, Nunes C, Amenitsch H, Reis S (2016a) Effects of resveratrol on the structure and fluidity of lipid bilayers: a membrane biophysical study. Soft Matter 12:2118–2126. https://doi.org/10.1039/C5SM02905H
Neves AR, Nunes C, Amenitsch H, Reis S (2016b) Resveratrol interaction with lipid bilayers: a synchrotron X-ray scattering study. Langmuir 32:12914–12922. https://doi.org/10.1021/acs.langmuir.6b03591
Neves AR, Nunes C, Reis S (2016c) Resveratrol induces ordered domains formation in biomembranes: Implication for its pleiotropic action. BBA-Biomembranes 1858:12–18. https://doi.org/10.1016/j.bbamem.2015.10.005
Ohvo-Rekilä H, Ramstedt B, Leppimäki P, Slotte JP (2002) Cholesterol interactions with phospholipids in membranes. Prog Lipid Res 41:66–97. https://doi.org/10.1016/s0163-7827(01)00020-0
Olas B, Holmsen H (2012) Interaction of resveratrol with membrane glycerophospholipids in model system in vitro. Food Chem Toxicol 50:4028–4034. https://doi.org/10.1016/j.fct.2012.07.066
Olbrich K, Rawicz W, Needham D, Evans E (2000) Water permeability and mechanical strength of polyunsaturated lipid bilayers. Biophys J 79:321–327. https://doi.org/10.1016/S0006-3495(00)76294-1
Orendorff CJ, Ducey MW Jr, Pemberton JE (2002) Quantitative correlation of Raman spectral indicators in determining conformational order in alkyl chains. J Phys Chem A 106:6991–6998. https://doi.org/10.1021/jp014311n

Pavan AR, Silva GDBd, Jornada DH, Chiba DE, Fernandes GFdS, Man Chin C, Dos Santos JL (2016) Unraveling the anticancer effect of curcumin and resveratrol. Nutrients 8:628. https://doi.org/10.3390/nu8110628

Phillips R, Ursell T, Wiggins P, Sens P (2009) Emerging roles for lipids in shaping membrane-protein function. Nature 459:379–385. https://doi.org/10.1038/nature08147

Quideau S, Deffieux D, Douat-Casassus C, Pouységu L (2011) Plant polyphenols: chemical properties, biological activities, and synthesis. Angew Chem Int Ed 50:586–621. https://doi.org/10.1002/anie.201000044

Ramassamy C (2006) Emerging role of polyphenolic compounds in the treatment of neurodegenerative diseases: a review of their intracellular targets. Eur J Pharmacol 545:51–64. https://doi.org/10.1016/j.ejphar.2006.06.025

Rosilio V (2018) How can artificial lipid models mimic the complexity of molecule–membrane interactions? Adv Biomembranes Lipid Self-Assembly. https://doi.org/10.1016/bs.abl.2017.12.004

Salehi B, Mishra AP, Nigam M, Sener B, Kilic M, Sharifi-Rad M, Fokou PVT, Martins N, Sharifi-Rad J (2018) Resveratrol: a double-edged sword in health benefits. Biomedicines 6:91. https://doi.org/10.3390/biomedicines6030091

Sarpietro MG, Spatafora C, Tringali C, Micieli D, Castelli F (2007) Interaction of resveratrol and its trimethyl and triacetyl derivatives with biomembrane models studied by differential scanning calorimetry. J Agric Food Chem 55:3720–3728. https://doi.org/10.1021/jf070070q

Shinoda K, Shinoda W, Mikami M (2008) Efficient free energy calculation of water across lipid membranes. J Comput Chem 29:1912–1918. https://doi.org/10.1002/jcc.20956

Stillwell W (2013) An introduction to biological membranes: from bilayers to rafts Newnes. Doi: https://doi.org/10.1016/B978-0-444-52153-8.00001-5

Stubbs CD, Smith AD (1984) The modification of mammalian membrane polyunsaturated fatty acid composition in relation to membrane fluidity and function. BBA-Rev. Biomembr 779:89–137. https://doi.org/10.1016/0304-4157(84)90005-4

Szlasa W, Zendran I, Zalesińska A, Tarek M, Kulbacka J (2020) Lipid composition of the cancer cell membrane. J Bioenerg Biomembr 52:1–22. https://doi.org/10.1007/s10863-020-09846-4

Tantipolphan R, Rades T, Strachan C, Gordon K, Medlicott N (2006) Analysis of lecithin–cholesterol mixtures using Raman spectroscopy. J Pharm Biomed 41:476–484. https://doi.org/10.1016/j.jpba.2005.12.018

Tosato MG, Girón JVM, Martin AA, Tippavajhala VK, de Mele MFL, Dicelio L (2018) Comparative study of transdermal drug delivery systems of resveratrol: high efficiency of deformable liposomes. Mater Sci Eng C 90:356–364. https://doi.org/10.1016/j.msec.2018.04.073

Truong VL, Jun M, Jeong WS (2018) Role of resveratrol in regulation of cellular defense systems against oxidative stress. BioFactors 44:36–49. https://doi.org/10.1002/biof.1399

Tsuchiya H, Nagayama M, Tanaka T, Furusawa M, Kashimata M, Takeuchi H (2002) Membrane-rigidifying effects of anti-cancer dietary factors. BioFactors 16:45–56. https://doi.org/10.1002/biof.5520160301

Van Meer G, Voelker DR, Feigenson GW (2008) Membrane lipids: where they are and how they behave. Nat Rev Mol Cell Biol 9:112–124. https://doi.org/10.1038/nrm2330

Vongsvivut J, Robertson EG, McNaughton D (2008) Surface-enhanced Raman scattering spectroscopy of resveratrol. Aust J Chem 61:921–929. https://doi.org/10.1071/CH08204

Wesołowska O, Kużdżał M, Štrancar J, Michalak K (2009) Interaction of the chemopreventive agent resveratrol and its metabolite, piceatannol, with model membranes. BBA-Biomembr 1788:1851–1860. https://doi.org/10.1016/j.bbamem.2009.06.005

White S (1977) Studies of the physical chemistry of planar bilayer membranes using high-precision measurements of specific capacitance. Ann NY Acad Sci 303:243–265

White S (1978) Formation of" solvent-free" black lipid bilayer membranes from glyceryl monooleate dispersed in squalene. Biophys J 23:337–347. https://doi.org/10.1016/S0006-3495(78)85453-8

Wood M, Morales M, Miller E, Braziel S, Giancaspro J, Scollan P, Rosario J, Gayapa A, Krmic M, Lee S (2021) Ibuprofen and the phosphatidylcholine bilayer: membrane water permeability in the presence and absence of cholesterol. Langmuir 37:4468–4480. https://doi.org/10.1021/acs.langmuir.0c03638

Yeagle P (1991) Modulation of membrane function by cholesterol. Biochimie 73:1303–1310. https://doi.org/10.1016/0300-9084(91)90093-g

Zalba S, Ten Hagen TL (2017) Cell membrane modulation as adjuvant in cancer therapy. Cancer Treat Rev 52:48–57. https://doi.org/10.1016/j.ctrv.2016.10.008

Publisher's Note Springer Nature remains neutral with regard to jurisdictional claims in published maps and institutional affiliations.